Model Order Reduction and Sensitivity Analysis for complex heat transfer simulations inside the human eyeball

Thomas Saigre, Christophe Prud'homme, Marcela Szopos

Séminaire EDP – IRMA
16th January 2024

Introduction

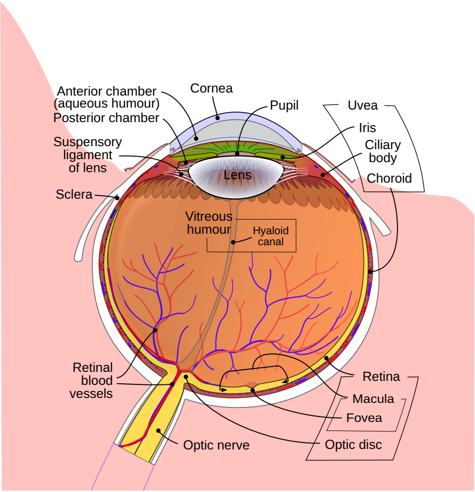

Rhcastilhos, from Wikipedia

- Need to understand ocular **physiology** and **pathology**,
- **Heat transfer** has an impact on the distribution of drugs in the eye[a],
- Complexity to perform **measurements** on a human subject[b], mostly available on surface[c].

[a] Bhandari et al., J. Control Release (2020)
[b] Rosenbluth et al., Exp. Eye Res. (1977)
[c] Purslow et al., Eye Contact Lens (2005)

Introduction

Model complexity

- Monophysics-Multiphysics problem
- Numerous parameters and scarce experimental data
- Influence of multiple risk factors or a combination of them

Introduction

Finite element

↓

In silico model

↕

Sensitivity analysis

Model complexity

- Monophysics-Multiphysics problem
- Numerous parameters and scarce experimental data
- Influence of multiple risk factors or a combination of them

Introduction

Validation of the model

In silico model

Model complexity

- Monophysics-Multiphysics problem
- Numerous parameters and scarce experimental data
- Influence of multiple risk factors or a combination of them

Sensitivity analysis

Prohibitive cost in 3D

Introduction

Validation of the model

Reduced basis method

In silico model

Model complexity

- Monophysics-Multiphysics problem
- Numerous parameters and scarce experimental data
- Influence of multiple risk factors or a combination of them

Model reduction

Sensitivity analysis

Prohibitive cost in 3D

Contents

General Framework: geometric, biophysical and parametrical models

Mathematical and computational framework

Numerical results

Sensitivity analysis

Conclusion

Geometrical model[1]

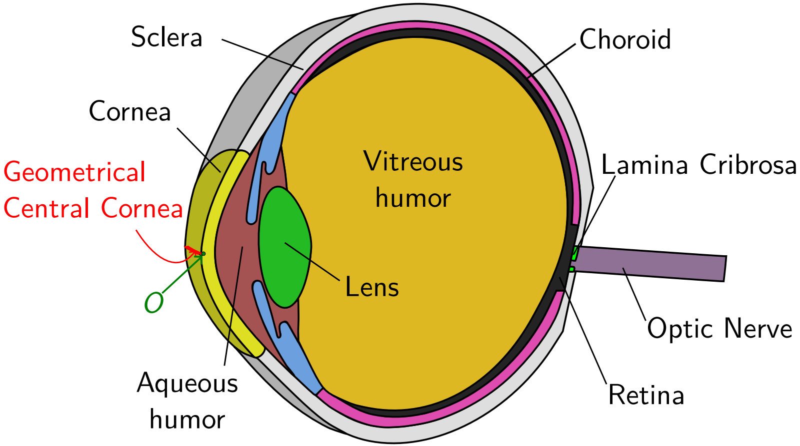

[1] Lorenzo Sala et al. "The ocular mathematical virtual simulator: A validated multiscale model for hemodynamics and biomechanics in the human eye". In: *International Journal for Numerical Methods in Biomedical Engineering* (), e3791.

Geometrical model: output of interest

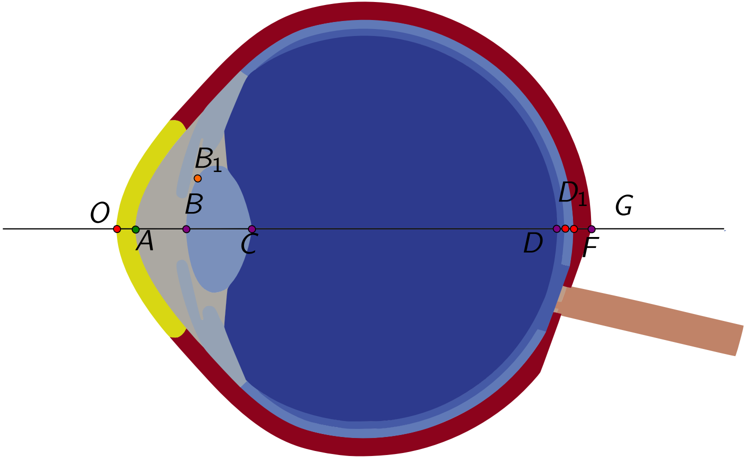

Biophysical model[1]

$$\nabla \cdot (k_i \nabla T_i) = 0 \qquad \text{on } \Omega = \bigcup_i \Omega_i$$

where :

- i is the region index (Cornea, Aqueous Humor, Vitreous Humor, Sclera, Iris, Lens, Choroid, Lamina, Retine, Optic Nerve),
- T_i [K] is the temperature in the volume i,
- k_i [$\mathrm{W\,m^{-1}}K^{-1}$] is the thermal conductivity.

[1] J.A. Scott. "A finite element model of heat transport in the human eye". In: *Physics in Medicine and Biology* 33.2 (1988), pp. 227–242; Ng, E.Y.K. and Ooi, E.H. "FEM simulation of the eye structure with bioheat analysis". In: *Computer Methods and Programs in Biomedicine* 82.3 (2006), pp. 268–276.

Biophysical model $\mathcal{E}_{\text{lin}}$

- Interface conditions : $\begin{cases} T_i = T_j \\ k_i(\nabla T_i \cdot \boldsymbol{n}_i) = -k_j(\nabla T_j \cdot \boldsymbol{n}_j) \end{cases}$ over $\partial\Omega_i \cap \partial\Omega_j$
- Robin condition on Γ_N : $-k\dfrac{\partial T}{\partial \boldsymbol{n}} = h_{\text{bl}}(T - T_{\text{bl}})$
- Linearized Neumann condition[a] on Γ_N :
  $$-k_i\frac{\partial T_i}{\partial \boldsymbol{n}} = h_{\text{amb}}(T_i - T_{\text{amb}}) + h_r(T_i - T_{\text{amb}}) + E$$

$h_r = 6\,\text{W}\,\text{m}^{-2}\,\text{K}^{-1}$

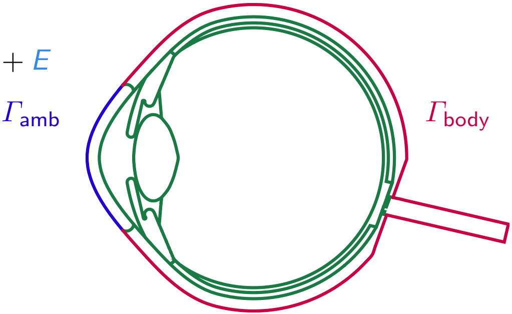

[a] J.A. Scott. "A finite element model of heat transport in the human eye". In: *Physics in Medicine and Biology* 33.2 (1988), pp. 227–242

Parameter dependent model

Symbol	Name	Dimension	Baseline value	Range
T_{amb}	Ambient temperature	[K]	298	[283.15, 303.15]
T_{bl}	Blood temperature	[K]	310	[308.3, 312]
h_{amb}	Ambient air convection coefficient	$[\mathrm{W\,m^{-2}\,K^{-1}}]$	10	[8, 100]
h_{bl}	Blood convection coefficient	$[\mathrm{W\,m^{-2}\,K^{-1}}]$	65	[50, 110]
E	Evaporation rate	$[\mathrm{W\,m^{-2}}]$	40	[20, 320]
k_{lens}	Lens conductivity	$[\mathrm{W\,m^{-1}\,K^{-1}}]$	0.4	[0.21, 0.544]
k_{cornea}	Cornea conductivity	$[\mathrm{W\,m^{-1}\,K^{-1}}]$	0.58	–
$k_{\text{sclera}} = k_{\text{iris}} = k_{\text{lamina}} = k_{\text{opticNerve}}$	Eye envelope components conductivity	$[\mathrm{W\,m^{-1}\,K^{-1}}]$	1.0042	–
$k_{\text{aqueousHumor}}$	Aqueous humor conductivity	$[\mathrm{W\,m^{-1}\,K^{-1}}]$	0.28	–
$k_{\text{vitreousHumor}}$	Vitreous humor conductivity	$[\mathrm{W\,m^{-1}\,K^{-1}}]$	0.603	–
$k_{\text{choroid}} = k_{\text{retina}}$	Vascular beds conductivity	$[\mathrm{W\,m^{-1}\,K^{-1}}]$	0.52	–
ε	Emissivity of the cornea	[–]	0.975	–

Geometrical parameters may be involved, but we will not consider them in this work.

Present work : focus on parameteric analysis

Parameter	Minimal value	Maximal value	Baseline value	Dimension
T_{amb}	283.15	303.15	298	[K]
T_{bl}	308.3	312	310	[K]
h_{amb}	8	100	10	$[\mathrm{W\,m^{-2}\,K^{-1}}]$
h_{bl}	50	110	65	$[\mathrm{W\,m^{-2}\,K^{-1}}]$
E	20	320	40	$[\mathrm{W\,m^{-2}}]$
k_{lens}	0.21	0.544	0.4	$[\mathrm{W\,m^{-1}\,K^{-1}}]$

Table 1: Range of values for the parameters

- We set $\mu = (T_{\mathrm{amb}}, T_{\mathrm{bl}}, h_{\mathrm{amb}}, h_{\mathrm{bl}}, E, k_{\mathrm{lens}}) \in D^{\mu} \subset \mathbb{R}^6$.
- $\bar{\mu} \in D^{\mu}$ is the baseline value of the parameters.

Mathematical and computational framework

Continuous and discrete problem

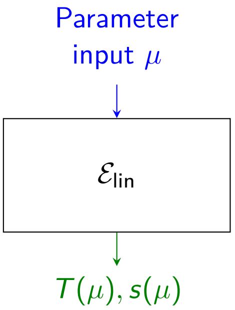

We set $V := H^1(\Omega)$.

Problem considered

Given $\mu \in D^\mu$, evaluate the output of interest

$$s(\mu) = \ell(T(\mu); \mu)$$

where $T(\mu) \in V$ is the solution of

$$a(T(\mu), v; \mu) = f(v; \mu) \quad \forall v \in V$$

The bilinear form $a(\cdot, \cdot; \mu)$ and the linear form $f(\cdot; \mu)$ are defined by the variational formulation of the problem.

Continuous and discrete problem

We set $V := H^1(\Omega)$

Para
inp

$\mathcal{E}$

$$a(T, v; \mu) = f(v; \mu)$$

with:

$$a(T, v; \mu) := k_{\text{lens}} \int_{\Omega_{\text{lens}}} \nabla T \cdot \nabla v \, \mathrm{d}x + \sum_{i \neq \text{lens}} k_i \int_{\Omega_i} \nabla T \cdot \nabla v \, \mathrm{d}x + \int_{\Gamma_{\text{amb}}} [h_{\text{amb}} T + h_r T] \, v \, \mathrm{d}\sigma + \int_{\Gamma_{\text{body}}} h_{\text{bl}} T v \, \mathrm{d}\sigma$$

$$f(v; \mu) := \int_{\Gamma_{\text{amb}}} [h_{\text{amb}} T_{\text{amb}} + h_r T_{\text{amb}} - E] \, v \, \mathrm{d}\sigma + \int_{\Gamma_{\text{body}}} h_{\text{bl}} T_{\text{bl}} v \, \mathrm{d}\sigma$$

$\boldsymbol{T}^{\text{fem}}(\mu), s(\mu)$

The bilinear form $a(\cdot, \cdot; \mu)$ and the linear form $f(\cdot; \mu)$ are defined by the variational formulation of the problem.

Continuous and discrete problem

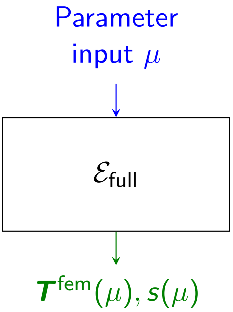

We set $V := H^1(\Omega)$. Denote by $V_h \subset V$ a finite-dimensional subspace of V of dimension $\mathcal{N}$.

High-fidelity model

Given $\mu \in D^\mu$, evaluate the output of interest

$$s(\mu) = \ell(\boldsymbol{T}^{\text{fem}}(\mu); \mu)$$

where $\boldsymbol{T}^{\text{fem}}(\mu) \in V_h$ is the solution of

$$a(\boldsymbol{T}^{\text{fem}}(\mu), v; \mu) = f(v; \mu) \quad \forall v \in V_h$$

The bilinear form $a(\cdot, \cdot; \mu)$ and the linear form $f(\cdot; \mu)$ are defined by the variational formulation of the problem.

Continuous and discrete problem

Parameter input μ

$$\downarrow$$

$$\boxed{\mathcal{E}_{\text{full}}}$$

$$\downarrow$$

$\boldsymbol{T}^{\text{fem}}(\mu), s(\mu)$

High fidelity resolution

Input: $\mu \in D^{\mu}$,

- Construct $\underline{\underline{\boldsymbol{A}}}(\mu)$, $\boldsymbol{f}(\mu)$ and $\boldsymbol{L}_k(\mu)$,
- Solve $\underline{\underline{\boldsymbol{A}}}(\mu)\boldsymbol{T}^{\text{fem}}(\mu) = \boldsymbol{f}(\mu)$,
- Compute outputs $s_k(\mu) = \boldsymbol{L}_k(\mu)^T\boldsymbol{T}^{\text{fem}}(\mu)$.

Output: Numerical solution $\boldsymbol{T}^{\text{fem}}(\mu)$ and outputs $s_k(\mu)$.

Model Order Reduction

- **Goal:** replicate input-output behavior of the high fidelity model $\mathcal{E}_{\mathrm{lin}}$ with a reduced order model $\mathcal{E}_{\mathrm{rbm}}$,
- With a procedure stable and efficient.

Parameter input μ

$\downarrow$

$\boxed{\mathcal{E}_{\mathrm{full}}(\mu)\ \text{(high fidelity)}}$

$\downarrow$

$T^{\mathrm{fem}}(\mu), s(\mu)$

Model Order Reduction

- **Goal:** replicate input-output behavior of the high fidelity model $\mathcal{E}_{\mathrm{lin}}$ with a reduced order model $\mathcal{E}_{\mathrm{rbm}}$,
- With a procedure stable and efficient.

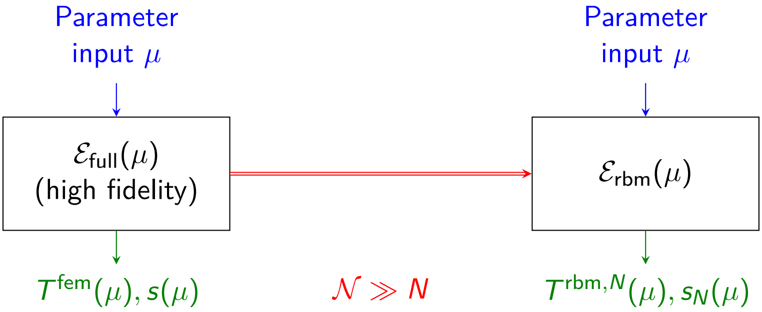

Reduced Basis Method[2]

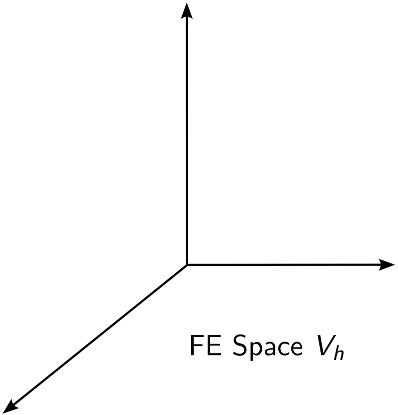

- High fidelity model: $\mathcal{E}_{\text{lin}} : \mu \mapsto T^{\text{fem}}(\mu)$,

[2] C. Prud'homme et al. "Reliable Real-Time Solution of Parametrized Partial Differential Equations: Reduced-Basis Output Bound Methods ". In: *Journal of Fluids Engineering* 124.1 (Nov. 2001), pp. 70–80.

Reduced Basis Method[2]

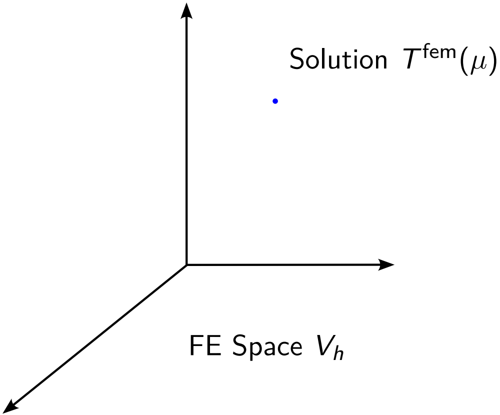

- High fidelity model: $\mathcal{E}_{\text{lin}} : \mu \mapsto T^{\text{fem}}(\mu)$,

[2] C. Prud'homme et al. "Reliable Real-Time Solution of Parametrized Partial Differential Equations: Reduced-Basis Output Bound Methods ". In: *Journal of Fluids Engineering* 124.1 (Nov. 2001), pp. 70–80.

Reduced Basis Method[2]

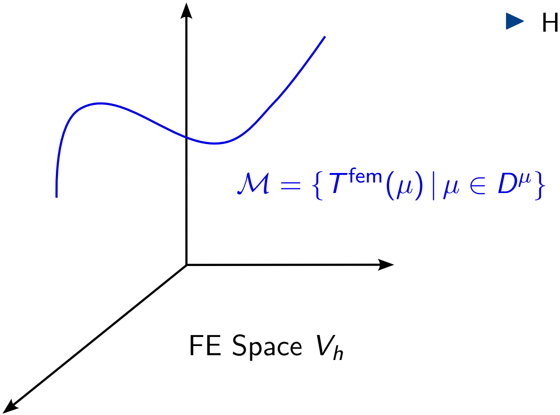

- High fidelity model: $\mathcal{E}_{\text{lin}} : \mu \mapsto T^{\text{fem}}(\mu)$,

[2] C. Prud'homme et al. "Reliable Real-Time Solution of Parametrized Partial Differential Equations: Reduced-Basis Output Bound Methods ". In: *Journal of Fluids Engineering* 124.1 (Nov. 2001), pp. 70–80.

Reduced Basis Method[2]

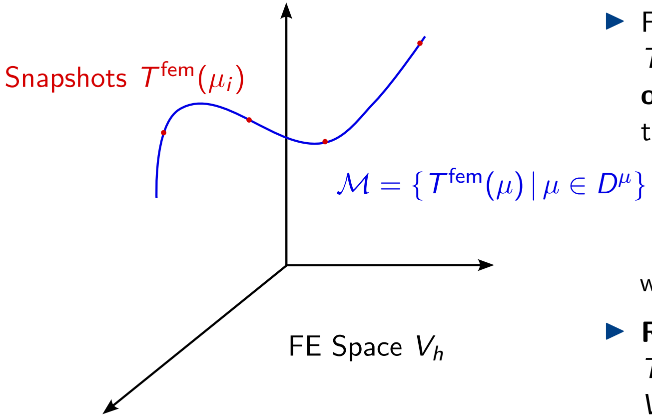

- From a set of **snapshots** $T^{\text{fem}}(\mu_1), \cdots, T^{\text{fem}}(\mu_N)$ computed **only once (*offline stage*)**, we define the **reduced functional space**:

$$V_N = \text{span}(\xi_1, \cdots, \xi_N)$$

where $\xi_i = T^{\text{fem}}(\mu_i)$, is orthonormalized.

- **Reduced solution (*online stage*):** $T^{\text{rbm},N}(\mu)$ solution of the PDE on V_N.

[2] C. Prud'homme et al. "Reliable Real-Time Solution of Parametrized Partial Differential Equations: Reduced-Basis Output Bound Methods ". In: *Journal of Fluids Engineering* 124.1 (Nov. 2001), pp. 70–80.

Reduced Basis Method

Problem considered

Given $\mu \in D^\mu$, evaluate the output of interest

$$s_N(\mu) = \ell(\boldsymbol{T}^{\text{rbm},N}(\mu); \mu)$$

where $\boldsymbol{T}^{\text{rbm},N}(\mu) \in V$ is the solution of

$$a(\boldsymbol{T}^{\text{rbm},N}(\mu), v; \mu) = f(v; \mu) \quad \forall v \in V_N$$

- *Snapshots matrix:* $\mathbb{Z}_N = [\xi_1, \cdots, \xi_N] \in \mathbb{R}^{\mathcal{N} \times N}$,

Reduced Basis Method

Problem considered

Given $\mu \in D^\mu$, evaluate the output of interest

$$s_N(\mu) = \ell(\boldsymbol{T}^{\text{rbm},N}(\mu);\mu)$$

where $\boldsymbol{T}^{\text{rbm},N}(\mu) \in V$ is the solution of

$$a(\boldsymbol{T}^{\text{rbm},N}(\mu), v;\mu) = f(v;\mu) \quad \forall v \in V_N$$

- *Snapshots matrix:* $\mathbb{Z}_N = [\xi_1, \cdots, \xi_N] \in \mathbb{R}^{\mathcal{N}\times N}$,
- Projection onto V_N: $\underline{\underline{\boldsymbol{A}}}_N(\mu) := \mathbb{Z}_N^T \underline{\underline{\boldsymbol{A}}}(\mu)\mathbb{Z}_N \in \mathbb{R}^{N\times N}$ and $\boldsymbol{f}_N(\mu) := \mathbb{Z}_N^T \boldsymbol{f}(\mu) \in \mathbb{R}^N$,

Reduced basis resolution

Input: $\mu \in D^\mu$,

- Construct $\underline{\underline{\boldsymbol{A}}}_N(\mu)$, $\boldsymbol{f}_N(\mu)$ and $\boldsymbol{L}_{N,k}(\mu)$,
- Solve $\underline{\underline{\boldsymbol{A}}}_N(\mu)\boldsymbol{T}^{\text{rbm},N}(\mu) = \boldsymbol{f}_N(\mu)$,
- Compute outputs $s_{N,k}(\mu) = \boldsymbol{L}_{N,k}(\mu)^T \boldsymbol{T}^{\text{rbm},N}(\mu)$.

Output: Numerical solution $\boldsymbol{T}^{\text{rbm},N}(\mu)$ and outputs $s_{N,k}(\mu)$.

Affine decomposition

- We want to write $\underline{\underline{\boldsymbol{A}}}(\mu) = \sum_{q=1}^{Q_a} \beta_A^q(\mu) \underline{\underline{\boldsymbol{A}}}^q$, and $\boldsymbol{F}(\mu) = \sum_{q=1}^{Q_f} \beta_F^q(\mu) \boldsymbol{F}^q$.
- Compute and store $\underline{\underline{\boldsymbol{A}}}_N^q = \underbrace{\mathbb{Z}_N^T \underline{\underline{\boldsymbol{A}}}^q \mathbb{Z}_N}_{\text{independent of } \mu}$ and $\boldsymbol{F}_N^q = \mathbb{Z}_N^T \boldsymbol{F}^q$.
- Hence $\underline{\underline{\boldsymbol{A}}}_N(\mu) = \sum_{q=1}^{Q_a} \beta_A^q(\mu) \underline{\underline{\boldsymbol{A}}}_N^q$ and $\boldsymbol{F}_N(\mu) = \sum_{q=1}^{Q_f} \beta_F^q(\mu) \boldsymbol{F}_N^q$.

Affine decomposition

- We want to write $\underline{\underline{\boldsymbol{A}}}(\mu) = \sum_{q=1}^{Q_a} \beta_A^q(\mu) \underline{\underline{\boldsymbol{A}}}^q$, and $\boldsymbol{F}(\mu) = \sum_{q=1}^{Q_f} \beta_F^q(\mu) \boldsymbol{F}^q$.
- Compute and store $\underline{\underline{\boldsymbol{A}}}_N^q = \mathbb{Z}_N^T \underline{\underline{\boldsymbol{A}}}^q \mathbb{Z}_N$ and $\boldsymbol{F}_N^q = \mathbb{Z}_N^T \boldsymbol{F}^q$.
- $a(T, v; \mu) = \sum_{q=1}^{4} \beta_A^q(\mu) a^q(T, v)$ with

$$
\begin{aligned}
\beta_A^1(\mu) &= k_{\text{lens}} & a^1(T, v) &= \int_{\Omega_{\text{lens}}} \nabla T \cdot \nabla v \,\mathrm{d}x \\
\beta_A^2(\mu) &= h_{\text{amb}} & a^2(T, v) &= \int_{\Gamma_{\text{amb}}} T v \,\mathrm{d}\sigma \\
\beta_A^3(\mu) &= h_{\text{bl}} & a^3(T, v) &= \int_{\Gamma_{\text{body}}} T v \,\mathrm{d}\sigma \\
\beta_A^4(\mu) &= 1 & a^4(T, v) &= \int_{\Gamma_{\text{amb}}} h_r T v \,\mathrm{d}\sigma + \sum_{i \neq \text{lens}} k_i \int_{\Omega_i} \nabla T \cdot \nabla v \,\mathrm{d}x
\end{aligned}
$$

Affine decomposition

- We want to write $\underline{\underline{\boldsymbol{A}}}(\mu) = \sum_{q=1}^{Q_a} \beta_A^q(\mu) \underline{\underline{\boldsymbol{A}}}^q$, and $\boldsymbol{F}(\mu) = \sum_{q=1}^{Q_f} \beta_F^q(\mu) \boldsymbol{F}^q$.
- Compute and store $\underline{\underline{\boldsymbol{A}}}_N^q = \mathbb{Z}_N^T \underline{\underline{\boldsymbol{A}}}^q \mathbb{Z}_N$ and $\boldsymbol{F}_N^q = \mathbb{Z}_N^T \boldsymbol{F}^q$.
- $f(v;\mu) = \sum_{p=1}^{2} \beta_F^p(\mu) f^p(v)$

$$\beta_F^1(\mu) = h_{\text{amb}} T_{\text{amb}} + h_r T_{\text{amb}} - E \qquad f^1(v) = \int_{\Gamma_{\text{amb}}} v \,\mathrm{d}\sigma$$

$$\beta_F^2(\mu) = h_{\text{bl}} T_{\text{bl}} \qquad f^2(v) = \int_{\Gamma_{\text{body}}} v \,\mathrm{d}\sigma$$

Offline / Online procedure

Offline:

- Solve N high-fidelity systems depending on $\mathcal{N}$ to form $\mathbb{Z}_N$,
- Form and store $\boldsymbol{F}_N^p(\xi_i)$
- Form and store $\underline{\underline{\boldsymbol{A}}}_N^q(\xi_i)$

Online: independant of $\mathcal{N}$

Given a new parameter $\mu \in D^\mu$,

- Form $\underline{\underline{\boldsymbol{A}}}_N(\mu)$: $O(Q_a N^2)$,
- Form $\boldsymbol{F}_N(\mu)$: $O(Q_f N)$,
- Solve $\underline{\underline{\boldsymbol{A}}}_N(\mu)\boldsymbol{T}^{\text{rbm},N}(\mu) = \boldsymbol{F}_N(\mu)$: $O(N^3)$,
- Compute $s_N(\mu) = \boldsymbol{L}_N(\mu)^T\boldsymbol{T}^{\text{rbm},N}(\mu)$: $O(N)$.

Error bound $\Delta_N(\mu)$

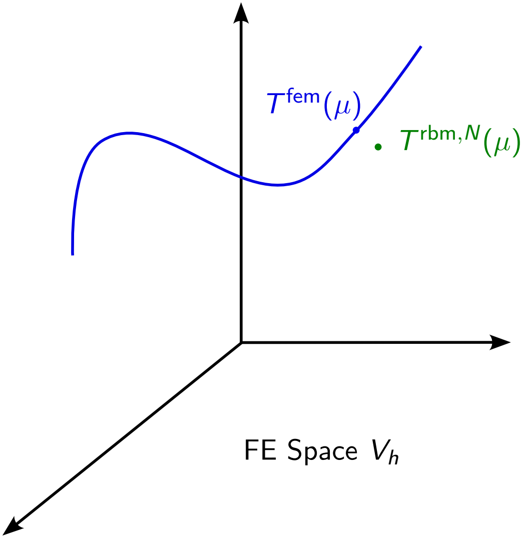

For $\mu \in D^\mu$, we define the error:

$$e(\mu) = \boldsymbol{T}^{\text{fem}}(\mu) - \boldsymbol{T}^{\text{rbm},N}(\mu)$$

Error bound $\Delta_N(\mu)$

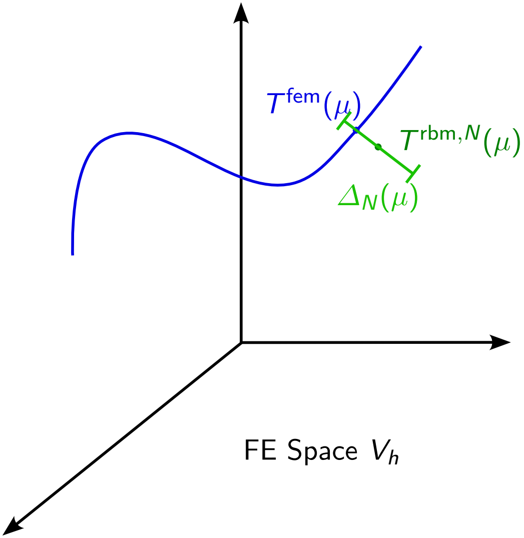

For $\mu \in D^\mu$, we define the error:

$$e(\mu) = \boldsymbol{T}^{\text{fem}}(\mu) - \boldsymbol{T}^{\text{rbm},N}(\mu)$$

We require this error bound to be:

- **rigorous**: $\|e(\mu)\|_X \leqslant \Delta_N(\mu)$,
- **sharp**: $\dfrac{\Delta_N(\mu)}{\|e(\mu)\|_X} \leqslant \eta_{\max}(\mu)$,
- **efficient**: the computation of $\Delta_N(\mu)$ does not depend on $\mathcal{N}$.

Error bound[3] $\Delta_N(\mu)$

Such an error bound can be constructed efficiently from the *residual* r of the variational problem:

$$r(v, \mu) := \ell(v; \mu) - a(T^{\mathrm{rbm},N}(\mu), v; \mu) \quad \forall v \in V$$

a lower bound $\alpha_{\mathrm{lb}}(\mu)$ of the coercivity constant $\alpha(\mu)$ of $a(\cdot, \cdot; \mu)$, and the affine decomposition of a and f:

$$\Delta_N^s(\mu) := \frac{\|r(\cdot, \mu)\|_{V'}^2}{\alpha_{\mathrm{lb}}(\mu)}$$

[3] C. Prud'homme et al. "Reliable Real-Time Solution of Parametrized Partial Differential Equations: Reduced-Basis Output Bound Methods ". In: *Journal of Fluids Engineering* 124.1 (Nov. 2001), pp. 70–80.

Non compliant problem

Definition

The problem is said to be *compliant* if the bilinear form a is symmetric, and $\ell = f$.

Error on the output

For $\mu \in D^\mu$, we have:

$$s(\mu) - s_N(\mu) = a(\boldsymbol{T}^{\text{fem}} - \boldsymbol{T}^{\text{rbm},N}, \boldsymbol{T}^{\text{fem}} - \boldsymbol{T}^{\text{rbm},N}; \mu)$$

$$|s(\mu) - s_N(\mu)| \leqslant \gamma(\mu) \left\| \boldsymbol{T}^{\text{fem}} - \boldsymbol{T}^{\text{rbm},N} \right\|_V^2$$

The error on the output converges as the square of the error on the field solution $\boldsymbol{T}^{\text{rbm},N}$

Non compliant problem

Definition

The problem is said to be *compliant* if the bilinear form a is symmetric, and $\ell = f$.

Error on the output

For $\mu \in D^\mu$, we have:

$$s(\mu) - s_N(\mu) = a(\boldsymbol{T}^{\text{fem}} - \boldsymbol{T}^{\text{rbm},N}, \boldsymbol{T}^{\text{fem}} - \boldsymbol{T}^{\text{rbm},N}; \mu)$$

$$|s(\mu) - s_N(\mu)| \leqslant \gamma(\mu) \left\| \boldsymbol{T}^{\text{fem}} - \boldsymbol{T}^{\text{rbm},N} \right\|_V^2$$

The error on the output converges as the square of the error on the field solution $\boldsymbol{T}^{\text{rbm},N}$

- Not our case ! We focus on output like $\ell(\mu) = \langle \delta_O, T(\mu) \rangle$

Non compliant problem

- We introduce the *dual problem*: Find $\psi(\mu) \in V$ such that:

$$a(v, \psi(\mu); \mu) = -\ell(v; \mu) \quad \forall v \in V$$

- We retrieve a similar property:

$$|s(\mu) - s_N(\mu)| \leqslant \gamma(\mu) \left\| T^{\text{fem}}(\mu) - T^{\text{rbm},N}(\mu) \right\|_V \left\| \psi^{\text{fem}}(\mu) - \psi^{\text{rbm},N}(\mu) \right\|_V$$

- The output error bound has the form:

$$\Delta_N^s(\mu) := \frac{\|r^{\text{pr}}(\cdot; \mu)\|_{V'}}{\sqrt{\alpha_{\text{lb}}(\mu)}} \frac{\|r^{\text{du}}(\cdot; \mu)\|_{V'}}{\sqrt{\alpha_{\text{lb}}(\mu)}}$$

Greedy algorithm

Algorithm 1: Greedy algorithm to construct the reduced basis.

Input: $\mu_0 \in D^\mu$, $\Xi_{\text{train}} \subset D^\mu$ and $\varepsilon_{\text{tol}} > 0$

$S \leftarrow [\mu_0]$;

while $\Delta_N^{\max} > \varepsilon_{tol}$ **do**

$\quad \mu^\star \leftarrow \arg\max_{\mu \in \Xi_{\text{train}}} \Delta_N(\mu)$ (and $\Delta_N^{\max} \leftarrow \max_{\mu \in \Xi_{\text{train}}} \Delta_N(\mu)$);

$\quad V_{N+1} \leftarrow \left\{ \boldsymbol{\xi} = \boldsymbol{T}^{\text{fem}}(\mu^\star) \right\} \cup V_N$;

$\quad$ Append $\mu^\star$ to S;

$\quad N \leftarrow N + 1$;

end

Output: Sample S, reduced basis V_N

Laplacian problem with Dirac as a right-hand side

We have a regular-enough domain $\Omega \subset \mathbb{R}^2$. Let $\boldsymbol{X}_0 = (x_0, y_0) \in \Omega$.
We consider the following problem:

$$\begin{cases} -\Delta u = \delta_{\boldsymbol{X}_0} & \text{in } \Omega \\ u = 0 & \text{on } \partial\Omega \end{cases} \tag{P_δ}$$

The finite element solution of Eq. (P_δ) $u_h \in V_h^k$ is defined as the solution of the following problem:

$$\int_\Omega \nabla u_h \cdot \nabla v_h = \langle \delta_{\boldsymbol{X}_0}, v_h \rangle \quad \text{for all } v_h \in V_h^k$$

Laplacian problem with Dirac as a right-hand side

We can compute the exact solution of Eq. (P_δ).

Definition: Let $G\colon \Omega \to \mathbb{R}$ be the *Green's function* defined by

$$G(x,y) = -\frac{1}{2\pi}\log\left(\sqrt{(x-x_0)^2+(y-y_0)^2}\right).$$

Proposition: This function satisfies $-\Delta G = \delta_{\boldsymbol{x}_0}$ in Ω

[4] Silvia Bertoluzza et al. "Local error estimates of the finite element method for an elliptic problem with a Dirac source term". In: *Numerical Methods for Partial Differential Equations* 34.1 (2018), pp. 97–120.

Laplacian problem with Dirac as a right-hand side

We can compute the exact solution of Eq. (P_δ).

Definition: Let $G\colon \Omega \to \mathbb{R}$ be the *Green's function* defined by

$$G(x, y) = -\frac{1}{2\pi} \log\left(\sqrt{(x - x_0)^2 + (y - y_0)^2}\right).$$

Proposition: This function satisfies $-\Delta G = \delta_{\boldsymbol{x}_0}$ in Ω

Theorem[4]**:** Under good conditions, involving subdomains $\Omega_0 \subset \Omega_1 \subset \Omega$, if u denotes the exact solution and u_h the finite element solution of the problem, then

$$\|u - u_h\|_{1,\Omega} \leqslant C(\Omega_0, \Omega_1, \Omega) h^k \sqrt{|\log(h)|}$$

[4] Silvia Bertoluzza et al. "Local error estimates of the finite element method for an elliptic problem with a Dirac source term". In: *Numerical Methods for Partial Differential Equations* 34.1 (2018), pp. 97–120.

Numerical results

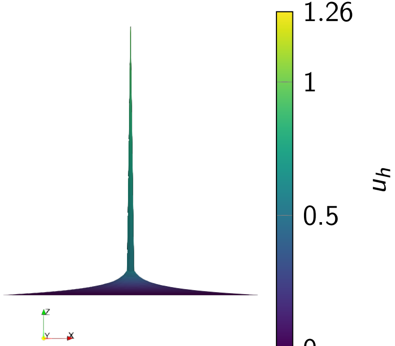

(a) Numerical solution u_h.

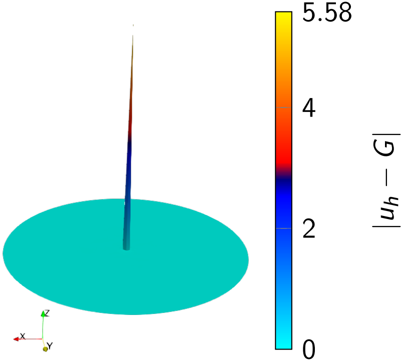

(b) Error on the numerical solution u_h compared to the exact solution G.

Convergence study

We compute the error over a domain $\Omega_0 = \Omega \setminus \overline{B(\boldsymbol{X}_0, r)}$ where $B(\boldsymbol{X}_0, r)$ is a ball centered in $\boldsymbol{X}_0$ and with radius r.

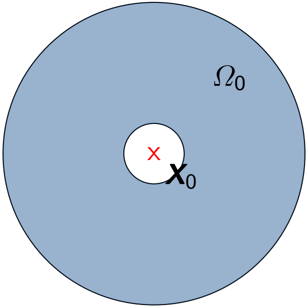

Error computed over Ω_0:

$$E := \|u - u_h\|_{L^2(\Omega_0)} \quad \text{or} \quad E := \|u - u_h\|_{H^1(\Omega_0)}$$

Convergence study: Mesh convergence

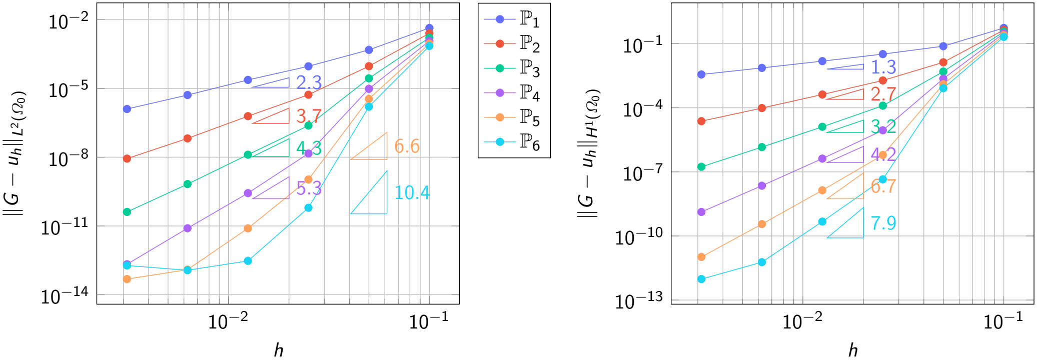

(c) $L^2(\Omega_0)$ (d) $H^1(\Omega_0)$

Convergence study: Position of the discontinuity to the border

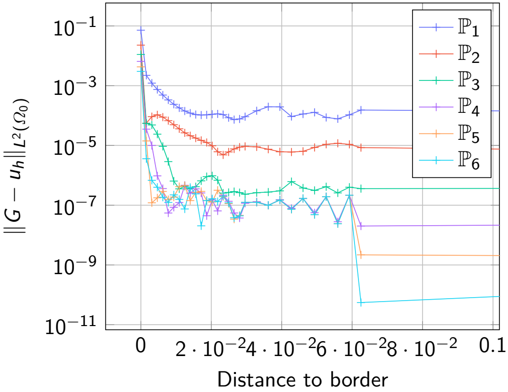

(e) $L^2(\Omega_0)$

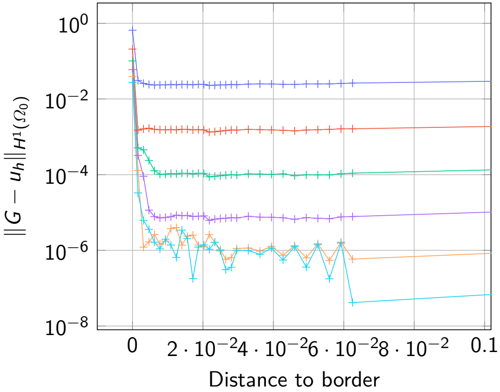

(f) $H^1(\Omega_0)$

Numerical results

High Fidelity model

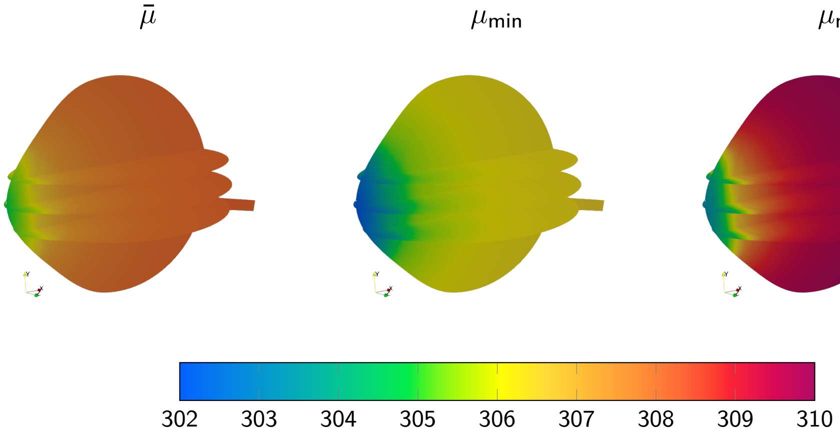

Figure 1: Distribution of the temperature [K] in the eyeball from the linear model $\mathcal{E}_{\mathrm{L}}(\mu)$.

Validation and comparison with previous studies

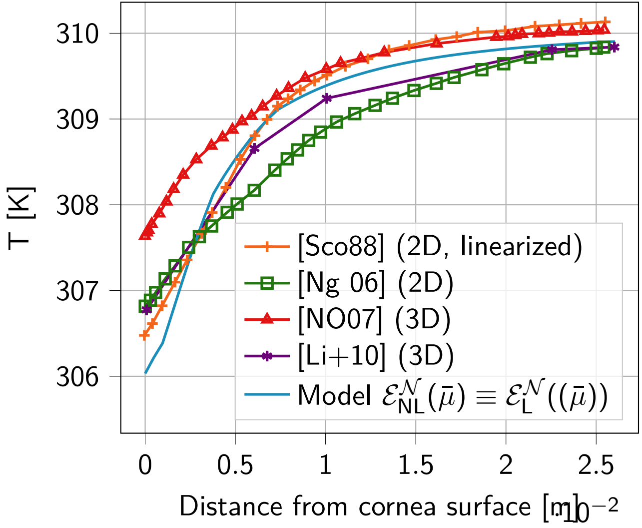

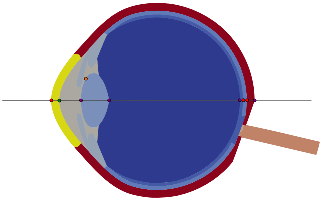

Validation: measured values over the GCC

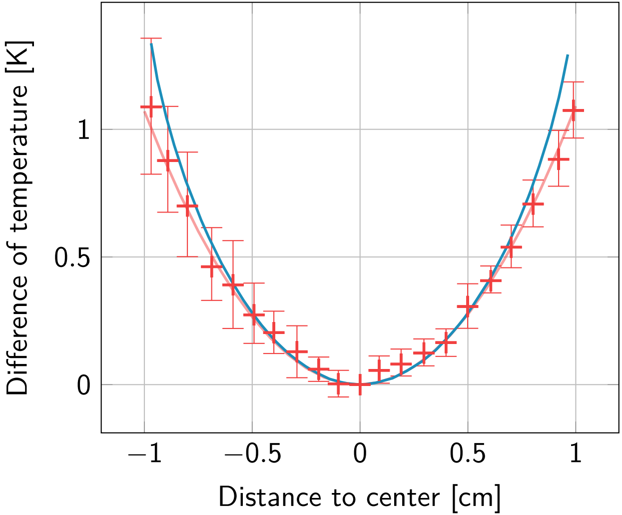

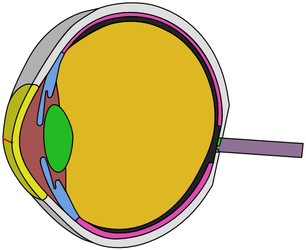

Time of execution

	Finite element resolution $T^{\text{fem}}(\mu)$			Reduced model $T^{\text{rbm},N}(\mu), \Delta_N(\mu)$
	$\mathbb{P}_1$	$\mathbb{P}_2$ (np=1)	$\mathbb{P}_2$ (np=12)	
Problem size	$\mathcal{N} = 207\ 845$	$\mathcal{N} = 1\ 580\ 932$		$N = 10$
t_{exec}	5.534 s	62.432 s	10.76 s	2.88×10^{-4} s
speed-up	11.69	1	5.80	$\mathbf{2.17 \times 10^5}$

Table 2: Times of execution, using mesh M3 for high fidelity simulations.

Results over a sampling $\Xi_{\text{test}} \subset D^\mu$ of 100 parameters

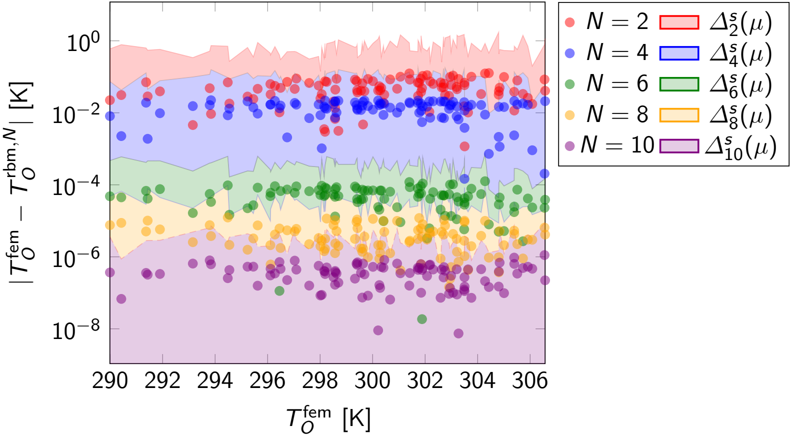

Figure 2: Error on RBM for various reduced basis sizes with error bound $\Delta_N(\mu)$.

Results over a sampling $\Xi_{\text{test}} \subset D^{\mu}$ of 100 parameters

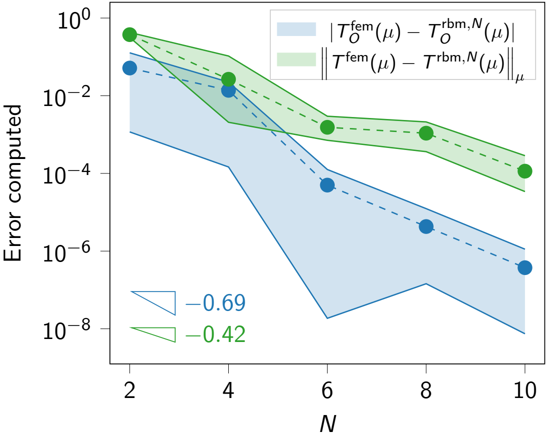

Figure 2: Convergence of the errors on the field and the output on point O.

Results over a sampling $\Xi_{\text{test}} \subset D^{\mu}$ of 100 parameters

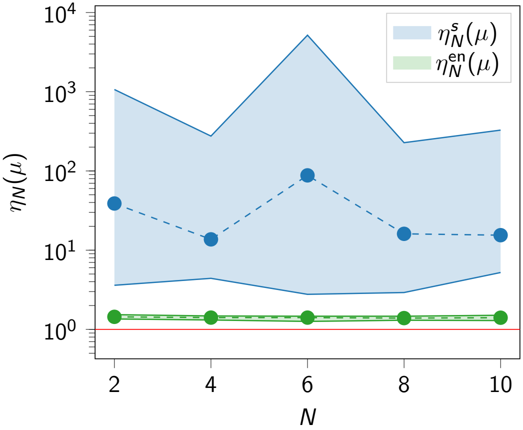

Figure 2: Stability of the effectivity.

Sensitivity analysis

Sobol indices

- $\mu = (\mu_1, \dots, \mu_n) \in D^\mu$,
- $\mu_i \sim X_i$ where $(X_i)_i$ is a family of **independent** random variables,
- Output $s_N(\mu) \sim Y = f(X_1, \dots, X_n)$,
- Distributions X_i selected from data available in the literature.

Sobol indices

- **First-order indices:** $S_j = \dfrac{\mathrm{Var}\left(\mathbb{E}\left[Y|X_j\right]\right)}{\mathrm{Var}(Y)}$ — effect of one parameter on the output
- **Total-order indices:** $S_j^{\mathrm{tot}} = \dfrac{\mathrm{Var}\left(\mathbb{E}\left[Y|X_{(-j)}\right]\right)}{\mathrm{Var}(Y)}$ — interaction of all parameters but one on the output

where $X_{(-j)} = (X_1, \dots, X_{j-1}, X_{j+1}, \dots, X_n)$.

Distributions

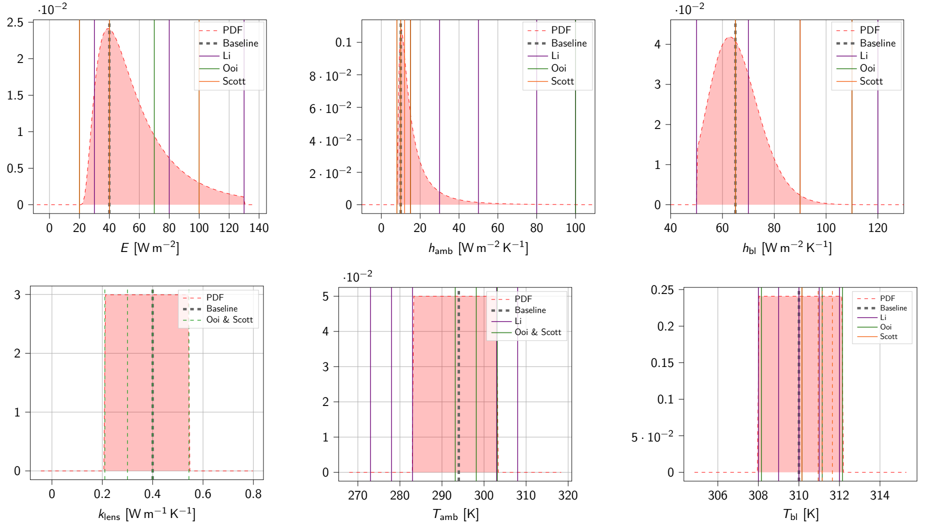

Uncertainty propagation

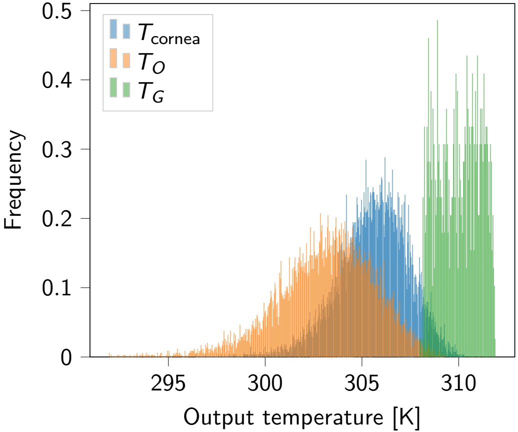

Figure 3: Distribution of the output, from the composed input distribution.

Stochastic sensitivity analysis

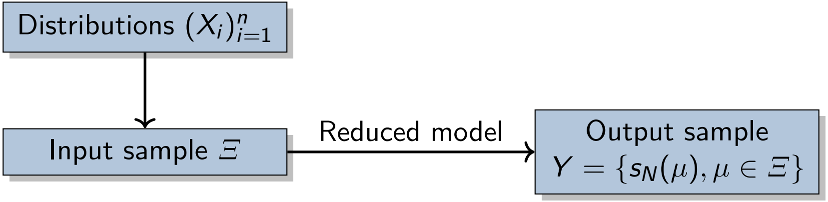

[5] Michaël Baudin et al. "OpenTURNS: An Industrial Software for Uncertainty Quantification in Simulation". In: *Handbook of Uncertainty Quantification*. Ed. by Roger Ghanem et al. Cham: Springer International Publishing, 2016, pp. 1–38.

Stochastic sensitivity analysis

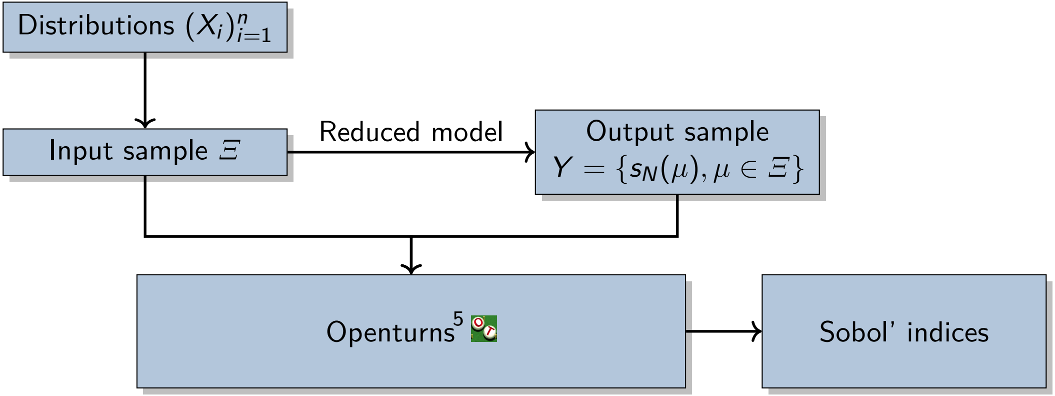

[5] Michaël Baudin et al. "OpenTURNS: An Industrial Software for Uncertainty Quantification in Simulation". In: *Handbook of Uncertainty Quantification*. Ed. by Roger Ghanem et al. Cham: Springer International Publishing, 2016, pp. 1–38.

Stochastic sensitivity analysis

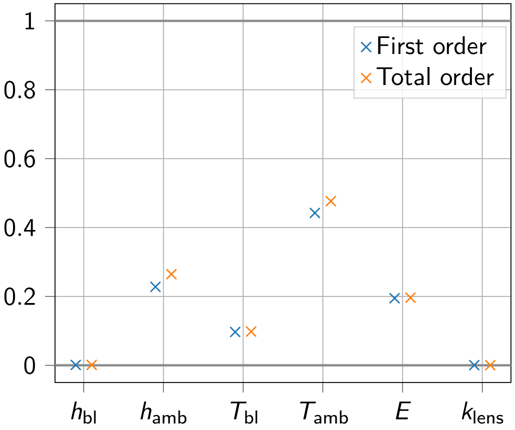

Figure 4: Sobol indices: temperature at point O.

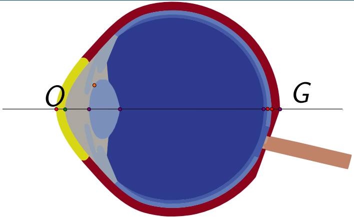

Temperature at the level of the **cornea**:

- **significantly** influenced by T_{amb}, h_{amb} (external factors) and E, T_{bl} (subject specific parameters) $\longrightarrow$ need for measurements/better model for these contributions,
- **minimally** influenced by k_{lens}, h_{bl} $\longrightarrow$ can be fixed at baseline value,
- **high order** interactions on T_{amb}, h_{amb}.

Stochastic sensitivity analysis

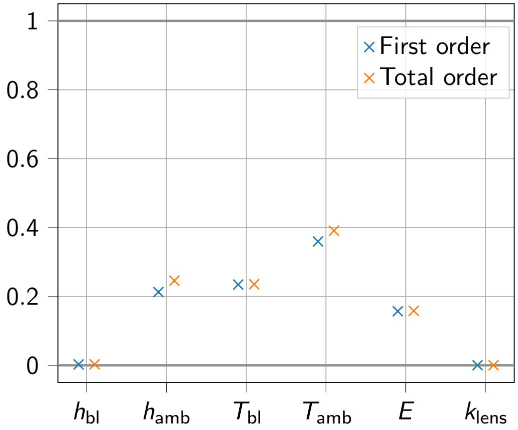

Figure 4: Mean temperature over the cornea.

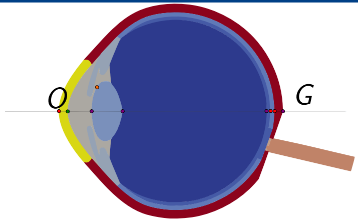

Mean temperature over the cornea:

- **significantly** influenced by T_{amb}, h_{amb} and E, T_{bl},
- **minimally** influenced by k_{lens}, h_{bl},
- **high order** interactions on T_{amb}, h_{amb}.

Stochastic sensitivity analysis

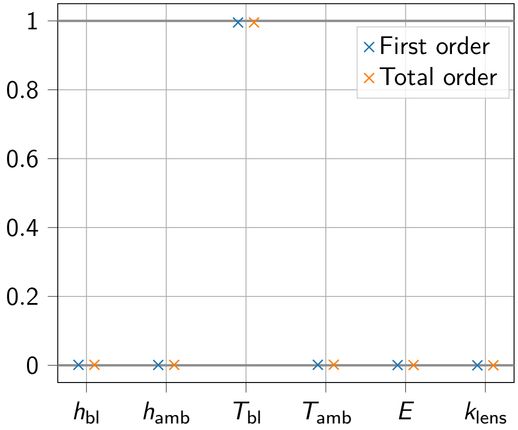

Figure 4: Sobol indices: temperature at point O.

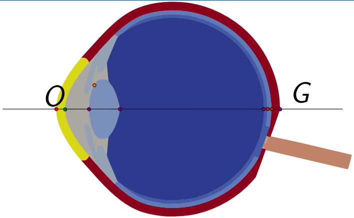

Temperature at the back of the eye:

- only influenced by the blood temperature.

Conclusion and outlook

- **Heat transport model in the human eye:** FEM simulations, validation against experimental data, and model order reduction,
- **Reduced model** with a **certified error bound**,
- **Sensitivity analysis:** computation of Sobol indices thanks to MOR, highlight of the impact of some parameters on the output.

Next steps:

- **Model:** couple thermal effect with aqueous humor dynamics in the anterior chamber,
- **Non intrusive** methods with zoom in zone of interest for non linear of non affine problems (EIM, NIRB),
- **Application:** robust framework to simulate drug delivery in the eye.

Conclusion and outlook

- **Heat transport model in the human eye:** FEM simulations, validation against experimental data, and model order reduction,
- **Reduced model** with a **certified error bound**,
- **Sensitivity analysis:** computation of Sobol indices thanks to MOR, highlight of the impact of some parameters on the output.

Next steps:

- **Model:** couple thermal effect with aqueous humor dynamics in the anterior chamber,
- **Non intrusive** methods with zoom in zone of interest for non linear of non affine problems (EIM, NIRB),
- **Application:** robust framework to simulate drug delivery in the eye.

Thank you for your attention!

Bibliography

[Bau+16] Michaël Baudin et al. "OpenTURNS: An Industrial Software for Uncertainty Quantification in Simulation". In: *Handbook of Uncertainty Quantification*. Ed. by Roger Ghanem, David Higdon, and Houman Owhadi. Cham: Springer International Publishing, 2016, pp. 1–38.

[BBS20] Ajay Bhandari, Ankit Bansal, and Niraj Sinha. "Effect of aging on heat transfer, fluid flow and drug transport in anterior human eye: A computational study". In: *Journal of Controlled Release* 328 (2020), pp. 286–303.

[Ber+18] Silvia Bertoluzza et al. "Local error estimates of the finite element method for an elliptic problem with a Dirac source term". In: *Numerical Methods for Partial Differential Equations* 34.1 (2018), pp. 97–120.

[EYB89] Nathan Efron, Graeme Young, and Noel A Brennan. "Ocular surface temperature.". In: *Current eye research* 8 9 (1989), pp. 901–6.

Bibliography

[Li+10] Eric Li et al. "Modeling and simulation of bioheat transfer in the human eye using the 3D alpha finite element method (αFEM)". In: *International Journal for Numerical Methods in Biomedical Engineering* 26.8 (2010), pp. 955–976.

[Ng 06] Ng, E.Y.K. and Ooi, E.H. "FEM simulation of the eye structure with bioheat analysis". In: *Computer Methods and Programs in Biomedicine* 82.3 (2006), pp. 268–276.

[NO07] E.Y.K. Ng and E.H. Ooi. "Ocular surface temperature: A 3D FEM prediction using bioheat equation". In: *Computers in Biology and Medicine* 37.6 (2007), pp. 829–835.

[Pru+01] C. Prud'homme et al. "Reliable Real-Time Solution of Parametrized Partial Differential Equations: Reduced-Basis Output Bound Methods ". In: *Journal of Fluids Engineering* 124.1 (Nov. 2001), pp. 70–80.

[PW05] Christine Purslow and James S Wolffsohn. "Ocular surface temperature: a review". en. In: *Eye Contact Lens* 31.3 (May 2005), pp. 117–123.

Bibliography

[QMN16] Alfio Quarteroni, Andrea Manzoni, and Federico Negri. *Reduced Basis Methods for Partial Differential Equations*. Springer International Publishing, 2016.

[RF77] Robert F. Rosenbluth and Irving Fatt. "Temperature measurements in the eye". In: *Experimental Eye Research* 25.4 (1977), pp. 325–341.

[Sal+] Lorenzo Sala et al. "The ocular mathematical virtual simulator: A validated multiscale model for hemodynamics and biomechanics in the human eye". In: *International Journal for Numerical Methods in Biomedical Engineering* (), e3791.

[Sco88] J.A. Scott. "A finite element model of heat transport in the human eye". In: *Physics in Medicine and Biology* 33.2 (1988), pp. 227–242.